Augmented obstacle avoidance controller design for mobile robots

Philipp Braun, Luca Zaccarian

Augmented obstacle avoidance controller design for mobile robots ⋆

Philipp Braun * **Luca Zaccarian** **

* *Research School of Electrical, Energy, and Materials Engineering, Australian National University (e-mail: philipp.braun@anu.edu.au)*
** *Dept. of Industrial Engineering, University of Trento & LAAS-CNRS, Université de Toulouse (e-mail: luca.zaccarian@laas.fr)*

Abstract: For unicycle robots and an arbitrary continuous reference tracking controller, we propose a control augmentation providing obstacle avoidance properties. The avoidance control law is activated in an eye-shaped neighborhood around an obstacle and guarantees that a specified domain around the obstacle is not entered. Switching between different control laws is orchestrated through a hybrid systems framework and Zeno behavior is avoided through appropriate hysteresis regions. Since the size of the eye-shaped neighborhood and its orientation depend continuously on the orientation and velocity of the robot, it can be guaranteed that the velocity input of the overall control law is continuous. Numerical simulations are provided to illustrate the performance of the tracking controller endowed with the avoidance augmentation.

Keywords: obstacle avoidance and reference tracking; controller design for hybrid systems

1. INTRODUCTION

Robot navigation, path planing and obstacle avoidance have been largely investigated in the past 20-30 years as well surveyed, for example, in Hoy et al. (2015); Sgorbissa and Zaccaria (2012). The corresponding algorithms are often classified in two families of *motion planning* and *reactive* algorithms, the latter ones essentially addressing unexpected or unplanned obstacle scenarios.

While many existing works address motion planning accounting for known obstacles, a system theoretic approach addressing avoidance of unexpected obstacles (the "reactive" paradigm) is rarely found in the literature, especially when seeking for rigorous guarantees of combined avoidance and target stabilization. Among other things, due to the bounded nature of obstacles, topological obstructions well commented in Sontag (1999) and Braun and Kellett (2020), among others, should be taken into account if wanting global guarantees associated with the avoidance algorithms.

An important field where this problem has been successfully addressed is that of collision avoidance in underwater systems (see Wiig et al. (2020, 2019) and references therein) and surface marine vessels (see Johansen et al. (2016) and references therein). Nonetheless, those approaches typically focus on smooth neighborhoods of the obstacle to be avoided (circles or spheres), thereby not directly addressing the hybrid (turn left or right) nature of the "avoidance" decision. A related approach is discussed in Chunyu et al. (2010), for example, where the authors switch between target set stabilizers and obstacle avoidance control laws when a ball around the obstacles is entered or left. While the approach is applicable to static and moving obstacles, the control law leads to chattering when the controller switches, which is avoided through the hybrid setting discussed here. Similarly, the papers Matveev et al. (2011) and Matveev et al. (2013) describe related approaches, where the robot travels with a constant speed and the input defining the angular velocity switches between tasks such as target set stabilization and obstacle avoidance. More closely related to our paradigm, Chen et al. (2017) uses barrier functions with a polytopic approach by taking into account acceleration constraints, which are not accounted for, in the simple suboptimal solution derived here.

In this paper we extend hybrid ideas from our previous work Braun et al. (2020) and Braun et al. (2019), augmenting an existing controller with an obstacle avoidance controller in a "reactive" fashion. The individual control laws are orchestrated through a hybrid systems framework to ensure that the overall system is well-defined and satisfies certain desirable properties in terms of absence of chattering and well-posed hybrid dynamics. Moreover, the controller preserves the properties of an arbitrary (predefined) tracking feedback, while the augmented avoidance controller only operates locally, close to the obstacle. Instead of discussing general linear systems as in Braun et al. (2020) and Braun et al. (2019), here, results on reference tracking and combined obstacle avoidance for unicycle models is addressed. Our avoidance controller is constructed based on barrier functions whose level sets resemble eye-shaped sets in form of a shell containing the obstacle in its interior. The shell changes its orientation with the orientation of the unicycle and the avoidance controller is activated based on the proximity to the obstacle and the velocity of the robot. Moreover, the shell size is scaled with the size of the forward velocity, so that a reasonable avoidance maneuver is enforced, depending on the traveling speed of the robot. Designing the controller based on a shell around the obstacle instead of a circle decreases the angle between the orientation of the unicycle

⋆ The research is supported in part by the Agence Nationale de la Recherche (ANR) via grant "Hybrid And Networked Dynamical sYstems" (HANDY), number ANR-18-CE40-0010.

and the tangent vectors on the boundary of the shell. This construction reduces the impact of switching between control laws and allows us to define a continuous forward velocity input even in cases where the hybrid controller switches from reference tracking to obstacle avoidance.

The paper is structured as follows. Section 2 introduces the setting and discusses the problem addressed in this paper. In Section 3 the avoidance neighborhood is made precise and the intuition behind the overall controller is explained before a rigorous derivation of the avoidance control law is given in Section 4. In Section 5 the controller is embedded in the hybrid systems framework before numerical results of the overall closed-loop system are illustrated in Section 6. The paper ends with concluding remarks in Section 7.

Throughout the paper, the following notation is used. The set $\{-1,+1\}$ is replaced by $\{\pm 1\}$. For $x \in \mathbb{R}^n$, $|\cdot|$ denotes the Euclidean norm, i.e., $|x| := \sqrt{x^\top x}$. For $\mathcal{A} \subset \mathbb{R}^n$ its closure is denoted by $\overline{\mathcal{A}}$. For $r > 0$ and $x \in \mathbb{R}^n$ we define $\mathcal{B}_r(x) := \{y \in \mathbb{R}^n |\ |y - x| < r\}$. In addition to the sign-function, which satisfies $\operatorname{sign}(0) = 0$ by assumption, we consider a slight variation of the form

$$s(r) \in \begin{cases} \operatorname{sign}(r), & \text{if } r \neq 0, \\ \{\pm 1\} = \{-1, 1\}, & \text{if } r = 0. \end{cases} \tag{1}$$

For $m \in \mathbb{R}_{\geq 0}$, the ensuing saturation is defined as

$$\operatorname{sat}^m(v) = \begin{cases} v, & \text{for } |v| \leq m, \\ \operatorname{sign}(v)m, & \text{for } |v| \geq m. \end{cases}$$

For $\phi \in \mathbb{R}$ and $\phi = \pi/2$ we consider the rotation matrices

$$R(\phi) = \begin{bmatrix} \cos(\phi) & -\sin(\phi) \\ \sin(\phi) & \cos(\phi) \end{bmatrix} \quad \text{and} \quad J = \begin{bmatrix} 0 & -1 \\ 1 & 0 \end{bmatrix}.$$

The matrix $R(\phi)$ satisfies $R(\phi)^{-1} = R(\phi)^\top = R(-\phi)$ and $R(\phi_1 + \phi_2) = R(\phi_1)R(\phi_2) = R(\phi_2)R(\phi_1)$ for all $\phi, \phi_1, \phi_2 \in \mathbb{R}$. The time derivative of $R(\phi)$ satisfies

$$\dot{R}(\phi) = \begin{bmatrix} -\sin(\phi) & -\cos(\phi) \\ \cos(\phi) & -\sin(\phi) \end{bmatrix} \dot{\phi} = R(\phi)J\dot{\phi} = JR(\phi)\dot{\phi}. \tag{2}$$

2. SETTING & PROBLEM FORMULATION

Consider the dynamics of a standard unicycle (see (Tzafestas, 2013, Section 2.3.1), for example)

$$\dot{x} = \begin{bmatrix} \dot{p}_1 \\ \dot{p}_2 \\ \dot{\phi} \end{bmatrix} = f(x,u) := \begin{bmatrix} v\cos(\phi) \\ v\sin(\phi) \\ w \end{bmatrix} = \begin{bmatrix} vR(\phi)\begin{bmatrix} 1 \\ 0 \end{bmatrix} \\ w \end{bmatrix} \tag{3}$$

with state $x := [p_1, p_2, \phi]^\top \in \mathbb{R}^3$ and input $u := [v, w]^\top \in \mathbb{R}^2$. Additionally, $p = [p_1, p_2]^\top$ is used to denote the position without the orientation ϕ in the following. By assumption, the inputs are bounded, i.e.,

$$v \in [-\bar{v}, \bar{v}], \quad w \in [-\bar{w}, \bar{w}] \quad \text{and} \quad \mathcal{U} := [-\bar{v}, \bar{v}] \times [-\bar{w}, \bar{w}]$$

for $\bar{v}, \bar{w} \in \mathbb{R}_{>0}$. The solution of (3) with respect to an initial condition $x_0 \in \mathbb{R}^3$ and input $u : \mathbb{R}_{\geq 0} \to \mathcal{U}$ is denoted by $t \mapsto x(t; x_0, u)$. If the initial condition and the input are clear from the context, they may be omitted.

Consider a tracking controller, ensuring that the robot follow a reference trajectory. While the results derived in this paper are independent of the specific tracking controller, we use in our simulation results a particular controller described in (Tzafestas, 2013, Section 5.4) as an example for the remainder of this paper. For a given input u_{ref} the reference signal is defined through a copy of the dynamics

$$\dot{x}_{\text{ref}} = f(x_{\text{ref}}, u_{\text{ref}}). \tag{4}$$

To obtain the control law, we introduce the error variables [1] $\tilde{x} = x - x_{\text{ref}}$ and the rotated error variables

$$\tilde{p}_{\text{rot}} = R(\phi)^\top \tilde{p}, \qquad \tilde{\phi}_{\text{rot}} = \tilde{\phi}. \tag{5}$$

With these definitions, for $k_1, k_2, k_\phi \in \mathbb{R}_{>0}$, the tracking controller used here is given by

$$u_{\text{tr}} = \begin{bmatrix} v_{\text{tr}} \\ w_{\text{tr}} \end{bmatrix} = \begin{bmatrix} -k_1\tilde{p}_{1,\text{ref}} + v_{\text{ref}}\cos(\tilde{\phi}_{\text{rot}}) \\ -k_\phi \sin(\tilde{\phi}_{\text{rot}}) - k_2 v_{\text{ref}}\tilde{p}_{2,\text{rot}} + w_{\text{ref}} \end{bmatrix}. \tag{6}$$

We refer to (Tzafestas, 2013, Section 5.4) for a derivation of the control law (6) and for its convergence properties. The control law (6) is not necessarily feasible. To obtain a feasible input with respect to $\mathcal{U}$ we consider the saturated tracking controller

$$u_{\text{ts}} = \begin{bmatrix} v_{\text{ts}} \\ w_{\text{ts}} \end{bmatrix} = \begin{bmatrix} \operatorname{sat}^{\bar{v}}(v_{\text{tr}}) \\ \operatorname{sat}^{\bar{w}}(w_{\text{tr}}) \end{bmatrix} \tag{7}$$

which is feasible by construction, coincides with (6) in the case $u_{\text{tr}} \in \mathcal{U}$ and preserves locally good convergence properties.

The control law (7) represents a generic tracking controller. The main contribution of this paper is to augment (7) with an avoidance controller that preserves asymptotically the properties of the original control law while, in addition, guaranteeing obstacle avoidance. The control laws are coordinated through a hybrid switching strategy. By design, the overall controller preserves certain continuity and robustness properties of the individual control laws and ensures that the avoidance controller acts only locally. The avoidance controller is discussed in detail in the following sections.

3. AVOIDANCE NEIGHBORHOODS & INTUITIVE CONTROLLER DESIGN

When the robot (3) is close to an obstacle, where "close to" is made mathematically precise later in this paper, the input u switches from the nominal tracking control law (7) to an avoidance controller. In this section we illustrate the neighborhood around the obstacle where this switching happens. Then, the core intuition behind the overall control law is explained.

3.1 The avoidance neighborhood

We consider obstacles centered at a point $c \in \mathbb{R}^2$ in the position plane p. Additionally, we consider two shifted points $c_q = c_q(\phi, \ell)$, $q \in \{\pm 1\}$, depending on the orientation ϕ and the time dependent length $\ell \in \mathbb{R}_{>0}$, which is adjusted online, depending on the magnitude of $|v_{\text{ts}}|$ of the speed commanded by the tracking controller, according to the following law

$$\ell(v_{\text{ts}}) := \max\left\{\ell_{\min}, \min\left\{\ell_{\max}, \tfrac{1}{\bar{w}}|v_{\text{ts}}|\right\}\right\}, \tag{8}$$

where $\ell_{\max} > \ell_{\min} > 0$ are some predefined bounds on the minimum and maximum shift, ensuring that $\ell \in [\ell_{\min}, \ell_{\max}]$.

Based on the selection of $\ell(v_{\text{ts}})$ in (8), points c_{+1} and c_{-1} are defined as

$$c_q := c - q\ell(v_{\text{ts}})R(\phi)\begin{bmatrix} 0 \\ 1 \end{bmatrix}, \qquad q \in \{\pm 1\}, \tag{9}$$

i.e., c_{+1} and c_{-1} are shifted versions of c rotated by ϕ and at a distance $|c - c_q| = |\ell(v_{\text{ts}})|$, $q \in \{\pm 1\}$ in the position p-plane (see Fig. 1).

[1] We deviate from the presentation in (Tzafestas, 2013, Section 5.4), which uses $\bar{x} = x_{\text{ref}} - x$ instead.

With the definition of c_q in (9), we introduce the barrier functions

$$B_q(x) := \tfrac{1}{2}|p - c_q|^2, \qquad q \in \{\pm 1\}, \tag{10}$$

which penalize the distance to c_q. The dependence of B_q on $\ell(v_{\text{ts}})$ is omitted for simplicity in definition (10). Fig. 1

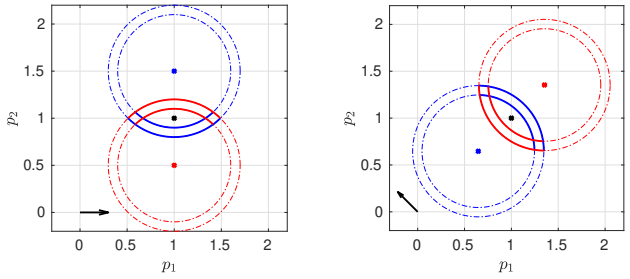

Fig. 1. Level sets of the functions B_{-1} (blue) and B_{+1} (red) for $c = [1, 1]^\top$, $\ell = \frac{1}{2}$ and $\phi = 0$ (left) and $\phi = \frac{3}{4}\pi$ (right). The robot is located at the origin with the orientation given by the arrow.

shows the level sets of B_q, $q \in \{\pm 1\}$ for $\phi = 0$ (left) and $\phi = \frac{3}{4}\pi$ (right), for the case $c = [1, 1]^\top$ and $\ell = \frac{1}{2}$.

The intersection of the sublevel sets of B_{+1} and B_{-1} forms an eye-shaped neighborhood of c resembling a shell. In particular, for any constant parametric "size" $s > 0$ satisfying $s \leq \ell_{\min}$, and any ϕ, ℓ, we define the shell

$$\mathcal{S}_s^\phi(\ell) := \left\{ p \in \mathbb{R}^2 \,\middle|\, B_q(x) \leq \tfrac{1}{2}(\ell + s)^2, \ \forall\, q \in \{\pm 1\} \right\}.$$

Moreover, for any pair of constant parameters r, s satisfying $0 < r < s \leq \ell_{\min}$, we define an inner and an outer shell with the properties $c \in \mathcal{S}_r^\phi(\ell) \subset \mathcal{S}_s^\phi(\ell) \subset \mathbb{R}^2$.

These two eye-shaped shells rule the hysteresis switching mechanism of our obstacle avoidance law. For a fixed $\phi \in \mathbb{R}$, define the functions $\eta_c^\phi, \delta_c^\phi : \mathbb{R}^2 \to \mathbb{R}$,

$$\begin{aligned} \eta_c^\phi(p) &= [\,0\ 1\,]\, R(\phi)^\top (p - c) \\ &= -\sin(\phi)(p_1 - c_1) + \cos(\phi)(p_2 - c_2), \end{aligned} \tag{11}$$

$$\begin{aligned} \delta_c^\phi(p) &= [\,1\ 0\,]\, R(\phi)^\top (p - c) \\ &= \cos(\phi)(p_1 - c_1) + \sin(\phi)(p_2 - c_2), \end{aligned} \tag{12}$$

the first one being zero on the longitudinal axis and the second one being zero on the lateral axis of the shell (see Fig. 2). Moreover, η_c^ϕ and δ_c^ϕ divide the (p_1, p_2)-plane in four quadrants.

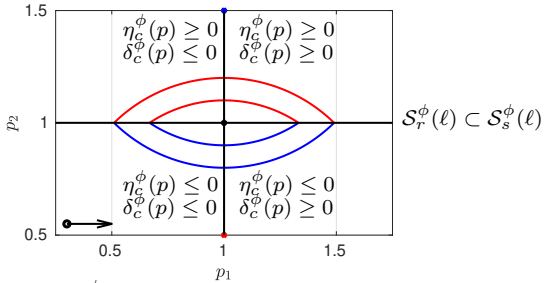

Fig. 2. While η_c^ϕ indicates whether the robot is at the left or the right of the obstacle, δ_c^ϕ indicates whether the obstacle is ahead or behind the robot. Additionally, the inner and outer shells $\mathcal{S}_r^\phi(\ell)$, $\mathcal{S}_s^\phi(\ell)$, for parameters $0 < r < s \leq \ell_{\min}$ are shown.

Before we continue with a rigorous definition of the avoidance control laws, we highlight connections between the definitions in this section leading to the intuition behind the avoidance controller. For $r > 0$ fixed, for all $\phi \in \mathbb{R}$, the shell $\mathcal{S}_r^\phi(\ell)$ (and thus also the obstacle itself) satisfies

$$\mathcal{S}_r^\phi(\ell) \subset \{p \in \mathbb{R}^2 |\ B_q(x) \leq \tfrac{1}{2}(\ell + r)^2\} \quad \forall\ q\ \in \{\pm 1\}.$$

Thus, if the initial state satisfies $p(0) \notin \mathcal{S}_r^{\phi(0)}(\ell)$ and $\phi(0) \in \mathbb{R}$, it is sufficient to guarantee that, on the correct boundary, we have

$$\langle \nabla B_q(x), f(x, u) \rangle \geq 0, \qquad q \in \{\pm 1\}, \tag{13}$$

for a suitable $q \in \{\pm 1\}$, to ensure that $p(t) \notin \mathcal{S}_r^\phi(\ell)$ for all $t \in \mathbb{R}_{\geq 0}$. Due to this reason, we characterize below the left-hand side of (13). We only focus on the case where $\ell(v_{\text{ts}})$ is constant, because we will clarify later that ℓ is held constant during the whole avoidance phase.

Lemma 1. Assume that $\ell = \bar{\ell} \in \mathbb{R}_{>0}$ is constant. Then, the gradient of B_q defined in (10) satisfies

$$\langle \nabla B_q(x), f(x, u) \rangle = (v - q\bar{\ell} w)\delta_c^\phi(p) \tag{14}$$

for $q \in \{\pm 1\}$. ⌟

Proof. Let $q \in \{\pm 1\}$ and $\bar{\ell} > 0$ be fixed. Since $R(\phi)^\top R(\phi) = I$, using (7), function $B_q(x)$ in (10) can be expressed as

$$\begin{aligned} B_q(x) &= \tfrac{1}{2}\left(p - c + q\bar{\ell} R(\phi)\,[\,0\,]\right)^\top \left(p - c + q\bar{\ell} R(\phi)\,[\,0\,]\right) \\ &= \tfrac{1}{2}(p - c)^\top (p - c) + \tfrac{1}{2}\bar{\ell}^2 + q\bar{\ell}\,(p - c)^\top R(\phi)\,[\,0\,]. \end{aligned}$$

Thus, using (2), it holds that

$$\begin{aligned} &\langle \nabla B_q(x), f(x, u) \rangle \\ &= \dot{p}^\top (p - c) + q\bar{\ell}\dot{p}^\top R(\phi)\,[\,0\,] + q\bar{\ell}\,(p - c)^\top R(\phi) J \dot{\phi}\,[\,0\,] \\ &= v \begin{bmatrix} \cos(\phi) \\ \sin(\phi) \end{bmatrix}^\top (p - c) + q\bar{\ell} v \begin{bmatrix} \cos(\phi) \\ \sin(\phi) \end{bmatrix}^\top \begin{bmatrix} -\sin(\phi) \\ \cos(\phi) \end{bmatrix} \\ &\quad + q\bar{\ell} w\,(p - c)^\top R(\phi) \begin{bmatrix} -1 \\ 0 \end{bmatrix} \\ &= (v - q\bar{\ell} w)\,[\,1\ 0\,]\, R(\phi)^\top (p - c) = (v - q\bar{\ell} w)\delta_c^\phi(p), \end{aligned}$$

which completes the proof. □

Based on (14), if the input (v, w) is selected so that $v - q\bar{\ell} w = 0$, then the distance between the robot and the point c_q is constant and the non-decrease condition (13) is satisfied. The following lemma motivates the definition of B_q, $q \in \{\pm 1\}$, and shows that (13) can be used to guarantee that a neighborhood around c is avoided.

Lemma 2. Let $r, \bar{\ell} \in \mathbb{R}_{>0}$, $q \in \{\pm 1\}$ and $u : \mathbb{R}_{\geq 0} \to \mathcal{U}$. Moreover, let $x_0 \in \mathbb{R}^3$ satisfy $B_q(x_0) \geq \frac{1}{2}(\bar{\ell} + r)^2$ and assume that $\frac{d}{dt} B_q(x(t; , x_0, u(t))) \geq 0$ for almost all $t \in \mathbb{R}_{\geq 0}$. Then $|p(t; x_0, u(t)) - c| \geq r$ for all $t \geq 0$. ⌟

Proof. It is sufficient to show that the set $\overline{\mathcal{B}}_r(c) \times \mathbb{R}$ is contained in the sublevel set $\{x \in \mathbb{R}^3 |\ B_q(x) \leq \frac{1}{2}(\bar{\ell} + r)^2\}$. Then the conditions on x_0 and on $p(\cdot; x_0, u(\cdot))$ ensure that $x(t; x_0, u(t)) \notin \overline{\mathcal{B}}_r(c) \times \mathbb{R}$ for all $t \geq 0$. An arbitrary element in $\overline{\mathcal{B}}_r(c)$ can be represented as $\tilde{p} = c + rR(\varphi)\,[\,1\,]$ for $\varphi \in \mathbb{R}$. Thus for $x = [\tilde{p}^\top, \phi]^\top$, $\phi \in \mathbb{R}$, with c_q as in (9), it holds that

$$\begin{aligned} &B_q(x) = \tfrac{1}{2}(\tilde{p} - c_q)^\top (\tilde{p} - c_q) \\ &= \tfrac{1}{2}(rR(\varphi)\,[\,1\,] + q\bar{\ell} R(\phi)\,[\,1\,])^\top (rR(\varphi)\,[\,1\,] + q\bar{\ell} R(\phi)\,[\,1\,]) \\ &= \tfrac{r^2}{2}\,[\,1\ 0\,]\, R(\varphi)^\top R(\varphi)\,[\,1\,] + \tfrac{\bar{\ell}^2}{2}\,[\,1\ 0\,]\, R(\phi)^\top R(\phi)\,[\,1\,] \\ &\quad + rq\bar{\ell}\,[\,1\ 0\,]\, R(\varphi)^\top R(\phi)\,[\,1\,] \leq \tfrac{r^2}{2} + \tfrac{\bar{\ell}^2}{2} + r\bar{\ell} = \tfrac{1}{2}(\bar{\ell} + r)^2 \end{aligned}$$

which completes the proof. □

3.2 Intuitive controller design

The controller proposed in this paper switches among three operating modes, with a hysteresis switching mechanism depending on the position p and the orientation ϕ. In particular, the first mode comprises the tracking controller

$u_{\rm ts}$ in (7), and the second and third mode comprise an avoidance controller $u_{\rm av}$ that can be split in an emergency mode $u_{\rm em}$ and a recovery mode $u_{\rm re}$.

A precise definition of the avoidance controller is derived in Section 4. Here we give an intuitive interpretation of the three control modes under the simplifying assumption that $v_{\rm ts} \geq 0$ (namely the tracking controller never moves backwards), to best deliver the message about the design intuition. In the actual control law of Sections 4 and 5, this simplification is not made.

Tracking mode. The tracking controller $u_{\rm ts}$ is active when $p \in \overline{\mathbb{R}^2 \backslash \mathcal{S}_s^\phi(\ell(v_{\rm ts}))}$ is satisfied. This implies that the obstacle does not affect the control input selection outside the outer shell $\mathcal{S}_s^\phi(\ell(v_{\rm ts}))$. ⌟

Emergency mode. Under the assumption that $v_{\rm ts} \geq 0$, the first avoidance mode corresponds to selection

$$v_{\rm av} := \text{sat}^{\bar{v}_w}(v_{\rm ts}), \qquad \bar{v}_w := \min\{\bar{v}, \bar{\ell}\bar{w}\} \tag{15}$$

$$u_{\rm em} = \begin{bmatrix} v_{\rm av} \\ q v_{\rm av}/\bar{\ell} \end{bmatrix}, \qquad \text{with} \quad q \in \{\pm 1\}, \tag{16}$$

where q is selected based on the position of the robot, i.e., if the robot is at the left or the right of the obstacle as depicted in Fig. 2. For $0 < r < s$, the emergency mode is activated when the inner shell $\mathcal{S}_r^\phi(\ell(v_{\rm ts}))$ is reached by the position p, and then $\ell(v_{\rm ts})$ is sampled and held as $\bar{\ell}$ and this mode remains active until the robot leaves the set $\{p \in \mathcal{S}_s^\phi(\bar{\ell}) |\ \delta_c^\phi(p) \leq 0\}$, namely with reference to Fig. 2 either the outer shell $\mathcal{S}_s^\phi(\bar{\ell})$ is left (and then the tracking mode is enabled) or the half-shell behind the obstacle is left the robot overtakes the obstacle so that $\delta_c^\phi(p) \geq 0$ (and the recovery mode is enabled).

Based on (14), we observe that the emergency mode (16) ensures that $\langle \nabla B_q(x), f(x, u_{\rm em}) \rangle = 0$ holds, while the saturation level $\bar{v}_w$ guarantees feasibility. Therefore the emergency mode ensures that the shell $\mathcal{S}_r^\phi(\bar{\ell})$ is never entered when the robot is heading towards the obstacle at the expense of sacrificing reference tracking. ⌟

Recovery mode. In this case $u_{\rm re}$ is defined as

$$u_{\rm re} = \begin{bmatrix} v_{\rm av} \\ \text{sat}^{v_{\rm av}/\bar{\ell}}(w_{\rm ts}) \end{bmatrix}, \tag{17}$$

where $v^\star$ is again defined in (15). Note that the recovery mode is independent of $q \in \{\pm 1\}$.

The recovery controller is activated when $\delta_c^\phi(p)$ changes its sign, i.e, when the obstacle is left behind and $\delta_c^\phi(p)$ becomes positive, while the robot is still within the outer shell. More precisely, the recovery mode remains active in the set $\{p \in \mathcal{S}_s^\phi(\bar{\ell}) |\ \delta_c^\phi(p) \geq 0\}$ and ensures that

$$\langle \nabla B_q(x), f(x, u_{\rm re}) \rangle \geq 0 \tag{18}$$

for all possible tracking inputs $(v_{\rm ts}, w_{\rm ts})$. Thus, in the worst case $\langle \nabla B_q(x), f(x, u_{\rm re}) \rangle = 0$ (obstacle avoidance) is guaranteed. Possibly, if $\langle \nabla B_q(x), f(x, u_{\rm re}) \rangle$ increases sufficiently over time, p will reach the set $\overline{\mathbb{R}^2 \backslash \mathcal{S}_s^\phi(\bar{\ell})}$ and the controller switches back to the tracking mode. ⌟

The switching among the different modes is made precise in Section 5 via a hybrid formalism Goebel et al. (2012). Before that, we describe more rigorously the avoidance control law, in the next section.

4. OBSTACLE AVOIDANCE CONTROLLER DESIGN

In this section we derive the avoidance controller $u_{\rm av}$. Along with the derivation we point out properties of the corresponding modes and motivate the particular input selections. Throughout this section, and during any avoidance maneuver, we freeze the parameter $\ell > 0$ to a constant value $\bar{\ell} > 0$ decided at the beginning of the emergency mode.

4.1 A minimally invasive avoidance control law

Based on the discussion so far, a justified approach for the design of the avoidance control law $u_{\rm av}$ is to consider the optimization problem

$$\begin{aligned} u^\star = \underset{u \in \mathcal{U}}{\text{argmin}}\ & \tfrac{1}{2}(v - v_{\rm ts})^2 + \tfrac{k}{2}(w - w_{\rm ts})^2 \\ \text{s.t. } & (v - q\bar{\ell}w)\delta_c^\phi(p) \geq 0, \end{aligned} \tag{19}$$

where $k \in \mathbb{R}_{>0}$ denotes a weighting factor and $u^\star = [v^\star, w^\star]^\top$ denotes the optimal solution depending on $(x, q, u_{\rm ts}) \in \mathbb{R}^3 \times \{\pm 1\} \times \mathbb{R}^2$.

Feasibility of the optimization problem (19) is trivially satisfied through $v = w = 0$. Moreover, since the objective function is strongly convex and the feasible domain is convex and compact for all $(x, q, u_{\rm ts})$ fixed, the optimal solution $u^\star$ is unique. The objective function penalizes the deviation from the nominal tracking controller and thus $u^\star$ can be considered to be minimally invasive. The constraints ensure that the input bounds $u^\star \in \mathcal{U}$ be satisfied and that the non-decrease condition (13) (see also (14)) be satisfied too.

While the solution of (19) implicitly defines a control law, an explicit expression of $u^\star$ can be obtained through quadratic multiparametric programming (Bemporad et al. (2002)). In particular, the inequality constraint capturing (13) can be replaced by

$$(v - qw\bar{\ell})\alpha \geq 0, \qquad \alpha \in \{0, \pm 1\}, \qquad q \in \{\pm 1\}, \tag{20}$$

depending on the sign $\alpha = \text{sign}(\delta_c^\phi(p))$. Then, under the assumption that α and q are fixed, the optimization problem (19) can be written in form of the quadratic multiparametric program

$$\begin{aligned} u_{q,\alpha}^\star = \underset{u \in \mathcal{U}}{\text{argmin}}\ & \tfrac{1}{2}(v - v_{\rm ts})^2 + \tfrac{k}{2}(w - w_{\rm ts})^2 \\ \text{s.t. } & \alpha v - (\alpha q \bar{\ell})w \geq 0, \end{aligned} \tag{21}$$

in the unknowns (v, w) and with parameters $(v_{\rm ts}, w_{\rm ts}) \in [-\bar{v}, \bar{v}] \times [-\bar{w}, \bar{w}]$. The multiparametric program (21) can be solved efficiently offline through Yalmip (Löfberg (2004)), and the Mult-Parametric Toolbox (Herceg et al. (2013)) in Matlab. To obtain an explicit expression of the optimal solution, (21) needs to be solved six times for all the possible values of $\alpha \in \{0, \pm 1\}$ and $q \in \{\pm 1\}$ and from the optimal solution computed offline the avoidance control law

$$\mu^q(x, u_{\rm ts}) = \begin{cases} u_{q,-1}^\star(u_{\rm ts}), \text{ if } \alpha = \text{sign}(\delta_c^\phi(p)) = -1, \\ u_{q,0}^\star(u_{\rm ts}), \text{ if } \alpha = \text{sign}(\delta_c^\phi(p)) = 0, \\ u_{q,+1}^\star(u_{\rm ts}), \text{ if } \alpha = \text{sign}(\delta_c^\phi(p)) = 1, \end{cases} \tag{22}$$

for $q \in \{\pm 1\}$, can be defined and stored. Control law (22) satisfies the following properties.

Lemma 3. For any $q \in \{\pm 1\}$ and any $\bar{\ell} > 0$, the feedback law (22) is a piecewise linear function of $(x, u_{\rm ts}) \in \mathbb{R}^3 \times \mathcal{U}$. Moreover, (22) is continuous at any point $(x, u_{\rm ts}) \in \mathbb{R}^3 \times \mathcal{U}$ satisfying $\delta_c^\phi(p) \neq 0$. ⌟

Proof. The result follows immediately from (Bemporad et al., 2002, Theorem 4.2). In particular, since (21) is a quadratic multiparametric program for α and q fixed,

$u^\star_{q,\alpha}(\cdot)$ is continuous and piecewise linear. This implies continuity of the control law μ^q, $q \in \{\pm 1\}$, whenever $\alpha \neq 0$, or equivalently $\delta^\phi_c(p) \neq 0$. □

Lemma 4. For $q \in \{\pm 1\}$ and $\bar{\ell} > 0$ consider an arbitrary tracking controller input $u_{\text{ts}} : \mathbb{R}_{\geq 0} \to \mathcal{U}$. Let $x_0 \in \mathbb{R}^3$ be such that $B_q(x_0) \geq \frac{1}{2}(\bar{\ell} + r)^2$ for $r > 0$ and let $x(\cdot; x_0, u_{\text{ts}})$ denote the closed-loop solution using the feedback law (22). Then, $|p(t; x_0, u_{\text{ts}}) - c| \geq r$ for all $t \in \mathbb{R}_{\geq 0}$. ⌟

Proof. The result follows from Lemma 2 and by design of the control law (22) whose constraints in (19) ensure condition (13). □

The control law (22) is well-defined for all pairs (x, u_{ts}). While in theory (22) has nice properties, i.e., the control law guarantees avoidance and is continuous for $x \in \mathbb{R}^3$ excluding a set of measure zero, numerically the control law may not behave well due its discontinuity at $[p^\top, \phi]^\top \in \mathbb{R}^3$ with $\delta^\phi_c(p) = 0$. In a numerical simulation $\delta^\phi_c(p) = 0$ is unlikely to be satisfied. One might argue that for $|\delta^\phi_c(p)|$ arbitrarily small the violation of the increase condition (13) is arbitrarily small and that $\{x \in \mathbb{R}^3 | \delta^\phi_c(p) = 0\}$ is only a set of measure zero. However, the optimal control law (22) may guarantee that $\frac{d}{dt} B(x(t)) = 0$ is satisfied for almost all $t \in [t_1, t_2]$ for a time interval defined through $t_2 > t_1 > 0$. Thus, in a numerical simulation, the control law (22) can lead to chattering where $\delta^\phi_c(x)$ changes its sign arbitrarily fast based on the numerical solver. To this end we propose a modification of (22) by considering suboptimal solutions of (19) guaranteeing additional regularity properties.

4.2 Enhanced avoidance controller design

To overcome the potential chattering problems of control law (22), as pointed out at the end of the previous section, we propose a modified and enhanced control law enjoying additional continuity properties at the cost of optimality. To this end, using the modified sign function $s(\cdot)$ in (1), introduce the triple $\kappa = [q, \alpha, \beta]^\top \in \{\pm 1\}^3$, which is initialized as follows at the beginning of each emergency mode:

$$\kappa^+ = \begin{bmatrix} q^+ & \alpha^+ & \beta^+ \end{bmatrix}^\top \in \begin{bmatrix} s(\eta^\phi_c(p)) & s(\delta^\phi_c(p)) & s(v_{\text{ts}}) \end{bmatrix}^\top \quad (23)$$

and has the following meaning, according to Fig. 2:

- q indicates whether the obstacle is being avoided from the left or the right;
- α indicates whether the robot is ahead or behind the obstacle;
- β indicates whether the robot is traveling forward or backwards.

Since the elements of κ are never zero by definition, this avoids the problems with the sets of measure zero where $\eta^\phi_c(p) = 0$, $\delta^\phi_c(p) = 0$ or $v_{\text{ts}} = 0$. Then, the case $\alpha = 0$ in the optimization problem (19) never occurs and, while input $u^\star_{q,\alpha}$ computed for $\alpha \in \{\pm 1\}$ might not be optimal for (21) when $\delta^\phi_c(p) = 0$, it still provides a feasible (suboptimal) solution.

Once the logic variables κ in (23) are initialized at the beginning of an avoidance maneuver, the avoidance direction remains unchanged until the robot exits the outer shell. In particular, both q and β are held constant during the whole avoidance phase (comprising the emergency and recovery modes). To this end, the first term $(v - v_{\text{ts}})^2$ of the cost function (21) is replaced by the term $(v - \beta|v_{\text{ts}}|)^2$. In this way, the heading speed v will never change sign, even in cases where the tracking control input v_{ts} changes sign. Of course when $v_{\text{ts}} > 0$ (positive forward speed) over the whole avoidance phase we recover the case discussed in Section 3.2. Ensuring that the heading speed never changes sign during the avoidance, also ensures that the avoidance direction q (left or right) remain unchanged.

A different strategy has to be followed for the evolution of variable α, which should switch only once (from -1 to $+1$ during forward motion and from $+1$ to -1 during backwards motion). To induce this behavior, looking at Fig. 2, when the robot approaches the obstacle with $v_{\text{ts}} > 0$, then $\delta^\phi_c(p)$ is initially negative and $\delta^\phi_c(p)$ increases until the obstacle is left behind. Similarly, if v_{ts} is negative, $\delta^\phi_c(p)$ decreases and eventually becomes negative. We can thus include an additional condition in the optimization problem (21) enforcing that $\beta \frac{d}{dt} \delta^\phi_c(p)$ be increasing. In particular, noting that

$$\begin{aligned} \tfrac{d}{dt}\delta^\phi_c(p) &= \dot{\phi}(-\sin(\phi))(p_1 - c_1) + \cos(\phi)\dot{p}_1 \\ &\quad + \dot{\phi}\cos(\phi)(p_2 - c_2) + \sin(\phi)\dot{p}_2 \\ &= w(\cos(\phi)(p_2 - c_2) - \sin(\phi)(p_1 - c_1)) \\ &\quad + \cos(\phi) v \cos(\phi) + \sin(\phi) v \sin(\phi) \\ &= \eta^\phi_c(p) w + v, \end{aligned}$$

then, the additional constraint

$$\beta \tfrac{d}{dt} \delta^\phi_c(p) = \beta(\eta^\phi_c(p) w + v) \geq 0 \quad (24)$$

ensures that $\delta_c(x)$ is either increasing or decreasing depending on the heading direction $\beta \in \{\pm 1\}$. Including this constraint in the optimization problem (19), with the modified cost function, we obtain the modified problem

$$\begin{aligned} u^\star = \underset{u \in \mathcal{U}}{\operatorname{argmin}} \; & \tfrac{1}{2}(v - \beta|v_{\text{ts}}|)^2 + \tfrac{k}{2}(w - w_{\text{ts}})^2 \\ \text{s.t. } & (v - q\bar{\ell} w)\alpha \geq 0, \quad (\eta^\phi_c(p) w + v)\beta \geq 0, \end{aligned} \quad (25)$$

for $q, \alpha, \beta \in \{\pm 1\}$. While feasibility and uniqueness of optimal solutions can be concluded as in the case of (19), due to the multiplication $\eta^\phi_c(p) w$, an explicit solution through quadratic multiparametric programming cannot be derived. Instead, we derive a suboptimal solution of (25) which guarantees that the velocity is continuous also across sign changes of α.

To this end, we choose suboptimal selections v_{av} and w_{av} sequentially. For $v^\star$ we consider

$$v_{\text{av}} = \underset{v \in [-\bar{v}, \bar{v}]}{\operatorname{argmin}} \; \tfrac{1}{2}(v - \beta|v_{\text{ts}}|)^2 \quad (26a)$$

$$\text{s.t. } (v + \bar{w}\bar{\ell}) \geq 0, \quad (v - \bar{w}\bar{\ell}) \leq 0 \quad (26b)$$

$$\beta v \geq 0, \quad (26c)$$

and for w_{av} we consider

$$w_{\text{av}} = \underset{w \in [-\bar{w}, \bar{w}]}{\operatorname{argmin}} \; \tfrac{1}{2}(w - w_{\text{ts}})^2 \quad (27a)$$

$$\text{s.t. } (v_{\text{av}} - q w \bar{\ell})\alpha \geq 0, \quad (27b)$$

$$\beta \eta^\phi_c(p) w \geq -|v^\star|, \quad (27c)$$

for $q, \alpha, \beta \in \{\pm 1\}$.

The optimization problem (26) is feasible since, for example, $v = 0$ satisfies the constraints. The constraints are defined in such a way that (13) holds by construction for $\alpha \in \{0, \pm 1\}$ and $q \in \{\pm 1\}$. In particular, (26b) guarantees that

$$(v_{\text{av}} + \bar{w}\bar{\ell}) \geq 0 \qquad \text{and} \qquad (v_{\text{av}} - \bar{w}\bar{\ell}) \leq 0,$$

giving w the authority to ensure that (27b), or equivalently the non-decrease condition in (19) be satisfied. Moreover,

observe that (26c), which is included to account for (24), is redundant because of the modified cost function involving the term $\beta|v_{\rm ts}|$. Then it follows that the optimal solution of (26) is given by

$$v_{\rm av} = \mathrm{sat}^{\bar v_w}(\beta|v_{\rm ts}|), \quad \bar v_w := \min\{\bar v, \bar w\ell\}, \tag{28}$$

which, in the case where $v_{\rm ts}$ is always positive (and therefore $\beta = 1$), reduces to (15) and the first components in (16) and (17). Note also that $v_{\rm av}$ is continuous (independent of $q, \alpha, \beta \in \{\pm 1\}$) and $v_{\rm av} = 0$ if and only $v_{\rm ts} = 0$.

For the optimization problem (27) we examine the inequality constraints (27b) and (27c), which, exploiting $v_{\rm av} = \beta|v_{\rm av}|$ for all $\beta \in s(v_{\rm av})$ and $q|\eta_c^\phi(p)| = \eta_c^\phi(p)$ for all $q \in s(\eta_c^\phi(p))$, can be written as

$$\alpha q w \le \alpha\beta|v_{\rm av}|/\bar\ell,\ -q\beta w \le \tfrac{|v_{\rm av}|}{|\eta_c^\phi(p)|},\ \ q, \alpha, \beta \in \{\pm 1\}. \tag{29}$$

Then, exploiting the fact that in the avoidance shell we have $|\eta_c^\phi(p)| \le s \le \ell_{\min} \le \bar\ell$, (29) is satisfied if the inequalities

$$\alpha q w \le \alpha\beta|v_{\rm av}|/\bar\ell,\ -q\beta w \le |v_{\rm av}|/\bar\ell,\ \ q, \alpha, \beta \in \{\pm 1\} \tag{30}$$

hold. This leads to the conditions

$$\begin{aligned} w &\le -|v_{\rm av}|/\bar\ell, && q \in \{\pm 1\},\ \alpha = q, && \beta = -q,\\ |w| &\le |v_{\rm av}|/\bar\ell, && q \in \{\pm 1\},\ \alpha \in \{\pm 1\},\ \beta = \alpha, \\ w &\ge |v_{\rm av}|/\bar\ell, && q \in \{\pm 1\},\ \alpha = -q, && \beta = q. \end{aligned} \tag{31}$$

Lemma 5. Consider the optimization problem (27), quantities $\bar v, \bar w \in \mathbb{R}_{>0}$, $\bar\ell \in [\ell_{\min}, \ell_{\max}]$, $v_{\rm ts} \in [-\bar v, \bar v]$ and $v^\star$ as defined in (28). Then (27) is feasible for all $q, \alpha, \beta \in \{\pm 1\}$, and all $x = (p, \phi) \in \mathbb{R}^3$ such that $p \in \mathcal{S}_s^\phi(\bar\ell)$. ⌟

Proof. Note that for $v_{\rm ts} = 0$ (i.e., $v_{\rm av} = 0$), $w = 0$ is feasible. Moreover, for $\eta_c^\phi(x) = 0$, (27c) is satisfied and the existence of $w \in [-\bar w, \bar w]$ satisfying (27b) is guaranteed through condition (26b). Thus, feasibility of (27) follows from the equivalent conditions (31), where we emphasize that $|v_{\rm av}|/\bar\ell \in [-\bar w, \bar w]$, due to the constraints (26b). □

Lemma 5 immediately implies the following result, completing the definition of the suboptimal avoidance controller.

Corollary 1. Consider the optimization problem (27), quantities $\bar v, \bar w \in \mathbb{R}_{>0}$, $\bar\ell \in [\ell_{\min}, \ell_{\max}]$, $v_{\rm ts} \in [-\bar v, \bar v]$ and $v_{\rm av}$ as defined in (28). For $x = (p, \phi) \in \mathbb{R}^3$ such that $p \in \mathcal{S}_s^\phi(\bar\ell)$,

$$w_{\rm av} = \begin{cases} \beta q|v_{\rm av}|/\bar\ell, & \text{if } q \in \{\pm 1\},\ \alpha = -\beta, \\ \mathrm{sat}^{|v_{\rm av}|/\bar\ell}(w_{\rm ts}), & \text{if } q \in \{\pm 1\},\ \alpha = \beta \end{cases} \tag{32}$$

defines a suboptimal solution of (27). ⌟

Note that combined with (28), the first condition of $w_{\rm av}$ capture the emergency control law (16), which must be active whenever $\alpha\beta = -1$, namely when approaching the obstacle, while the second condition captures the recovery controller (17), which must be active after overtaking the obstacle, with $\alpha\beta = 1$.

The following statement summarizes the properties of the avoidance controller (emergency + recovery) developed in the past sections. Its proof follows immediately from the results proven in the section.

Proposition 1. For any $q, \beta \in \{\pm 1\}$ and any $\bar\ell \in [\ell_{\min}, \ell_{\max}]$, an arbitrary tracking controller input $u_{\rm ts} : \mathbb{R}_{\ge 0} \to \mathcal{U}$ and any initial condition $x_0 = (p_0, \phi_0)$ such that p belongs to the closure of $\mathcal{S}_s^\phi(\bar\ell) \setminus \mathcal{S}_r^\phi(\bar\ell)$, the avoidance control law $u = u_{\rm av} := (v_{\rm av}, w_{\rm av})$ as defined in (28) and (32) ensures that the ensuing trajectory $t \mapsto p(t)$ satisfies $|p(t) - c| \ge r$ for all $t \in [0, T]$, where T is the smallest time such that $p(T)$ belongs to the boundary of $\mathcal{S}_s^\phi(\bar\ell)$. ⌟

Intuitively speaking, Proposition 1 ensures that the robot does not hit the obstacle. Note that no stronger statement can be concluded due to the fact that we make essentially no assumption on the nature of the tracking controller, which could possibly aim (in a worst case scenario) exactly at the obstacle. Providing stronger statements under more restrictive conditions on the tracking controller and the position of the obstacle is regarded as future work.

5. THE HYBRID CONTROL ARCHITECTURE

We present in this section a hybrid formulation of the tracking controller augmented with the avoidance (emergency+recovery) augmentation proposed here, adopting the notation in Goebel et al. (2012). The presented formulation provides convenient hysteresis switching among the different operating modes. The hybrid state of the closed loop comprises the plant state $x = (p, \phi)$, the memory variable $\bar\ell \in [\ell_{\min}, \ell_{\max}]$ and the logic variables $\kappa = [q, \alpha, \beta]^\top$ already introduced in (23), with the novelty that, while $\alpha, \beta \in \{\pm 1\}$, we extend the domain of q to be $q \in \{0, -1, +1\}$, to associate the tracking motion to the selection $q = 0$. Summarizing, the hybrid state is selected as

$$\xi := (x, \bar\ell, \kappa) \in \Xi := \mathbb{R}^3 \times [\ell_{\min}, \ell_{\max}] \times \{-1, 0, 1\} \times \{\pm 1\}^2,$$

and the overall hybrid dynamics can be summarized by

$$\dot\xi = \begin{bmatrix} \dot x \\ \dot{\bar\ell} \\ \dot\kappa \end{bmatrix} = \begin{bmatrix} f(x, \gamma(\xi, u_{\rm ts}) \\ 0 \\ 0 \end{bmatrix}, \quad \xi \in \mathcal{C} := \overline{\Xi \setminus \mathcal{D}}, \tag{33a}$$

$$\xi^+ = \begin{bmatrix} x^+ \\ \bar\ell^+ \\ \kappa^+ \end{bmatrix} \in \begin{bmatrix} x \\ G(\xi, u_{\rm ts})) \end{bmatrix}, \qquad \xi \in \mathcal{D}. \tag{33b}$$

which is a hybrid system with jump and flow dynamics affected by the external input $u_{\rm ts}$, which stems from any arbitrary tracking controller. Following the intuition of Section 3.2 and the derivations of Section 4, in the proximity of the obstacle, the jump set $\mathcal{D}$ allows for a mode transition among three possible modes: *tracking*, with $q = 0$, *emergency*, with $|q| = 1$ and $\alpha\beta = -1$, and *recovery*, with $|q| = 1$ and $\alpha\beta = 1$, while the flow set $\mathcal{C}$ is selected as the closed complement of this jump set. Accordingly, input $u = \gamma(\xi, u_{\rm ts})$ is selected as follows:

$$\gamma(\xi, u_{\rm ts}) := \begin{cases} u_{\rm ts}, & \text{if } \ q = 0, \\ u_{\rm em} = \begin{bmatrix} v_{\rm av} \\ \beta q|v_{\rm av}|/\bar\ell \end{bmatrix}, & \text{if } \ \begin{matrix} |q| = 1, \\ \alpha\beta = -1 \end{matrix} \\ u_{\rm re} = \begin{bmatrix} v_{\rm av} \\ \mathrm{sat}^{|v_{\rm av}|/\bar\ell}(w_{\rm ts}) \end{bmatrix}, & \text{if } \ \begin{matrix} |q| = 1, \\ \alpha\beta = 1 \end{matrix} \end{cases} \tag{34}$$

where, according to (28), $v_{\rm av} = \mathrm{sat}^{\bar v_w}(\beta|v_{\rm ts}|)$ and $\bar v_w := \min\{\bar v, \bar w\ell\}$.

Concerning the jumps (mode transitions) of hybrid system (33), three jump sets capture the transition diagram represented in Figure 3, namely

$$\mathcal{D} := \mathcal{D}_{\rm tr} \cup \mathcal{D}_{\rm em} \cup \mathcal{D}_{\rm re} \tag{35}$$

$$\mathcal{D}_{\rm tr} := \{\xi \in \Xi : |q| = 1, p \in \overline{\mathbb{R}^2 \setminus \mathcal{S}_s^\phi(\bar\ell)}\}, \tag{36}$$

$$\mathcal{D}_{\rm em} := \{\xi \in \Xi : q = 0, p \in \mathcal{S}_r^\phi(\ell(v_{\rm ts}))\} \tag{37}$$

$$\mathcal{D}_{\rm re} := \{\xi \in \Xi : |q| = 1, \alpha\delta_c^\phi(p) \le 0, \alpha\beta = -1\} \tag{38}$$

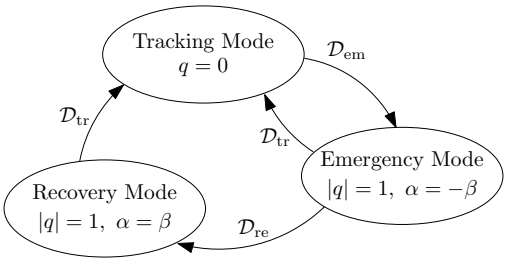

Fig. 3. Mode transitions induced by the jumps of (33).

Intuitively speaking, jumps from $\mathcal{D}_{\text{tr}}$ occur from outside the outer shell (or at the boundary) when the avoidance mode is active ($|q| = 1$); jumps from $\mathcal{D}_{\text{em}}$ occur when the tracking mode is active ($q = 0$) and the robot hits the inner shell, while jumps from $\mathcal{D}_{\text{re}}$ occur when the emergency controller is active ($|q = 1|$ and $\alpha\beta = -1$ and the robot overtakes the obstacle). The corresponding jump laws are issued from (23) and are given by

$$G(\xi, u_{\text{ts}}) = \bigcup_{i \in \{\text{tr,em,re}\}: \xi \in \mathcal{D}_i} g_i(\xi, u_{\text{ts}}) \tag{39}$$

$$g_{\text{tr}} := \begin{bmatrix} \bar{\ell} \\ 0 \\ \alpha \\ \beta \end{bmatrix}, \ g_{\text{em}} := \begin{bmatrix} g_\ell(x, v_{\text{ts}}) \\ s(\eta_c^\phi(p)) \\ -s(v_{\text{ts}}) \\ s(v_{\text{ts}}) \end{bmatrix}, \ g_{\text{re}} := \begin{bmatrix} \bar{\ell} \\ q \\ \beta \\ \beta \end{bmatrix},$$

$$g_\ell(x, v_{\text{ts}}) := \min\{|p - c_{s(\eta_c^\phi(p))}| - r, \ell(v_{\text{ts}})\}, \tag{40}$$

where we omitted the dependence of $g_{\text{tr}}, g_{\text{em}}, g_{\text{re}}$ on (ξ, u_{ts}) to keep the notation compact. While g_{tr} is quite intuitive because it merely ensures that $q^+ = 0$ to enable the tracking mode, the transition g_{em} to emergency mode structurally ensures $\alpha^+\beta^+ = -1$ and, if $\alpha^+ \notin s(\delta_c^\phi(p))$, an immediate further jump from $\mathcal{D}_{\text{re}}$ (according to g_{re}) ensures that the recovery mode is correctly triggered by swapping the sign of α.

As a final step we discuss the update law for the state $\bar{\ell}$ in (39), related to the size of the outer shell. In particular, during free motion, as per (37), the outer shell is related to $\ell(v_{\text{ts}})$, as defined in (8), which depends on the velocity v_{ts}. Intuitively this makes sense. Indeed, if v_{ts} is large, the robot needs to react early to guarantee avoidance without abrupt maneuvers. In contrast if v_{ts} is small, the size of the shell can be reduced.

When the avoidance starts, the parameter $\bar{\ell}$ is frozen as per the corresponding term in g_{em}, in (39), because the avoidance controller requires a constant parameter $\bar{\ell}$. In particular, function g_ℓ in (40) ensures that $\bar{\ell}$ is small enough so that the position p never falls in the interior of the inner shell. The first term in the minimum is only relevant in the case that the system jumps from the recovery mode to the tracking mode and immediately to the emergency mode.

Remark 1. The last term in (8) is used to ensure that the velocity is typically continuous when the control law switches from the tracking to the emergency mode (unless the situation just described occurs). In particular, using the definition of $\ell(v_{\text{ts}})$ in $\bar{v}_w$ defined in (28), it holds that

$$\begin{aligned} \bar{v}_w &= \min\left\{\bar{v}, \bar{w} \cdot \max\left\{s, \tfrac{1}{\bar{w}}|v_{\text{ts}}(t)|\right\}\right\} \\ &= \min\left\{\bar{v}, \max\left\{\bar{w}s, |v_{\text{ts}}(t)|\right\}\right\} \end{aligned}$$

which implies that

$$\bar{v}_w = |v_{\text{ts}}(t)| \leq \bar{v} \qquad \text{if} \quad |v_{\text{ts}}(t)| \leq \bar{w}s \quad \text{and}$$

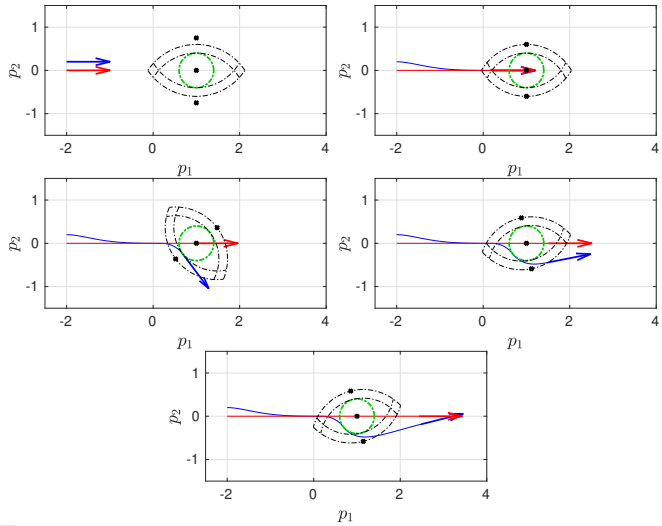

Fig. 4. Trajectory of the unicycle (blue) tracking the reference signal (red) while avoiding a neighborhood around $c = [1, 0]^\top$. The figures show the beginning and the end of the simulation as well as the times when the controller switches.

$$|v_{\text{ts}}(t)| \leq \bar{v}_w = \min\{\bar{v}, \bar{w}s\} \quad \text{if} \quad |v_{\text{ts}}(t)| \geq \bar{w}s.$$

In both cases, the avoidance control law in (28) satisfies $v_{\text{av}} = v_{\text{ts}}$, and thus, the overall control law is continuous when switching from $q = 0$ to $q \in \{\pm 1\}$. ∘

By construction, the closed loop (33) guarantees avoidance of the neighborhood $\mathcal{B}_r(c)$ with additional tracking properties depending on the selection of u_{ts}. Moreover, due to the hysteresis region $\mathcal{S}_s^\phi(\bar{\ell}) \backslash \mathcal{S}_r^\phi(\bar{\ell})$, $0 < r < s$ and the non-decrease condition $\frac{d}{dt}\delta_c^\phi(p) \geq 0$, the switching dynamics avoids Zeno behavior and chattering. A rigorous analysis of combined avoidance and tracking properties of (33) using a specific tracking controller is left for future work. Instead we illustrate the overall controller through numerical simulations in the next section.

6. NUMERICAL SIMULATIONS

We analyze the performance of the augmented avoidance controller based on numerical simulations. We use the parameters $\bar{v} = \bar{w} = 2$. The parameters of the reference tracking controller (6), (7) are set to $k_1 = k_2 = k_\phi = 5$. The obstacle is centered at $c = [1, 0]^\top$ and the inner and the outer shell are defined through $r = 0.4$ and $s = 0.6$. All simulations are initialized outside the shell with $q = 0$. For the results in Fig. 4 and Fig. 5 the reference input $u_{\text{ref}} = [\frac{1}{2}\cos(t) + 1, 0]^\top$ is used while the results in Fig. 6 are obtained through $u_{\text{ref}} = [1.5, -1]^\top$.

Fig. 4 shows the trajectory of the unicycle (blue) and the reference system (4) (red) in the (p_1, p_2)-plane at the beginning of the simulation, the end of the simulation and whenever the controller switches among the different modes as per Fig. 3. While the reference signal hits the obstacle c, the unicycle avoids the neighborhood $\mathcal{B}_{0.4}(c) = \mathcal{B}_r(c)$ by deviating via the emergency mode. The corresponding control law is visualized in Fig. 5. Observe that the velocity input is continuous in this example. As discussed, this is not necessarily the case when the control law switches from u_{av} to u_{ts}.

Fig. 6 shows the closed-loop solution (right) of the unicycle (blue) and the reference signal (4) (red) for different initial conditions (left). The reference signal describes a circular motion passing through the obstacle c, while the

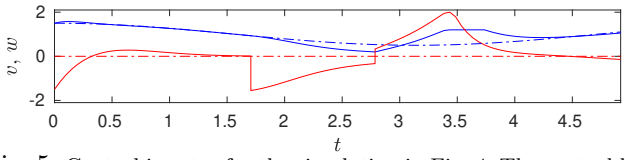

Fig. 5. Control input u for the simulation in Fig. 4. The control law (34) (v in blue, w in red) is shown using a solid line while u_{ref} is shown using a dashed line.

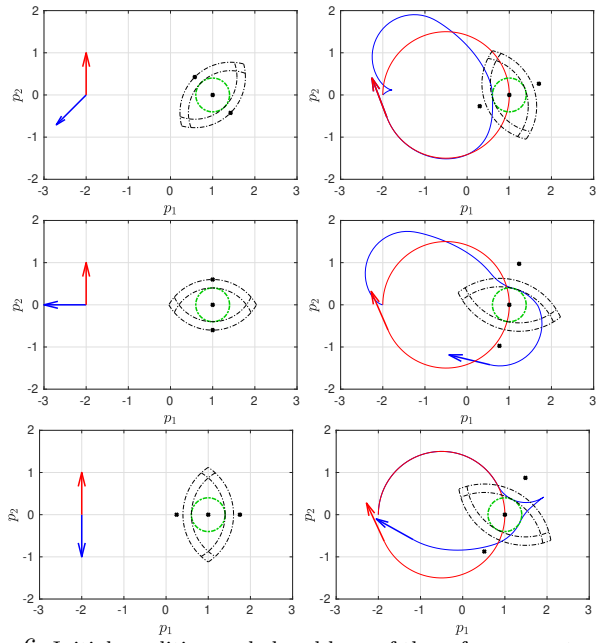

Fig. 6. Initial condition and closed loop of the reference system (3) (red), and the avoidance-augmented closed loop (33), (blue).

controller successfully avoids $\mathcal{B}_{0.4}(c)$ independent of the initial conditions. For a longer simulation, the three closed-loop solutions converge to the same solution while in the transient the avoidance strategy depends on the initial condition. Since the avoidance controller v_{av} does not change its sign while it is active, the sign is only changed after the outer shell is left, leading to the kink in the bottom right illustration in Fig. 6, interestingly showing the avoidance phases for this specific scenario.

7. CONCLUSIONS

In this paper, based on a given reference tracking controller, an augmented obstacle avoidance controller has been derived. The two control laws are combined using the hybrid systems framework such that the overall controller guarantees avoidance of a neighborhood around obstacles while preserving properties of the tracking controller away from the obstacle. The avoidance controller is derived using barrier functions whose level sets resemble a shell containing the obstacle and providing a suboptimal solution of a minimally invasive optimization problem. By changing the orientation and the size of the shell with the heading and the velocity of the robot it is guaranteed that the velocity input is continuous. Future work will concentrate on a rigorous analysis of the closed loop system in terms of robust avoidance and tracking performance. Additionally, the ideas will be extended to more realistic unicycle models with $\dot{u}$ as input to guarantee that v and w are continuous.

REFERENCES

Bemporad, A., Morari, M., Dua, V., and Pistikopoulos, E.N. (2002). The explicit linear quadratic regulator for constrained systems. *Automatica*, 38(1), 3–20.

Braun, P., Kellett, C.M., and Zaccarian, L. (2019). Uniting control laws: On obstacle avoidance and global stabilization of underactuated linear systems. In *Proc. of the IEEE Conference on Decision and Control*, 8154–8159.

Braun, P., Kellett, C.M., and Zaccarian, L. (2020). Explicit construction of stabilizing robust avoidance controllers for linear systems with drift. *IEEE Transactions on Automatic Control*. doi:10.1109/TAC.2020.2986730.

Braun, P. and Kellett, C.M. (2020). Comment on "Stabilization with guaranteed safety using control Lyapunov–barrier function". *Automatica*, 122, 109225.

Chen, Y., Peng, H., and Grizzle, J. (2017). Obstacle avoidance for low-speed autonomous vehicles with barrier function. *IEEE Transactions on Control Systems Technology*, 26(1), 194–206.

Chunyu, J., Qu, Z., Pollak, E., and Falash, M. (2010). Reactive target-tracking control with obstacle avoidance of unicycle-type mobile robots in a dynamic environment. In *Proc. of the American Control Conference*, 1190–1195.

Goebel, R., Sanfelice, R.G., and Teel, A.R. (2012). *Hybrid Dynamical Systems: Modeling, Stability, and Robustness*. Princeton University Press.

Herceg, M., Kvasnica, M., Jones, C., and Morari, M. (2013). Multi-Parametric Toolbox 3.0. In *Proc. of the European Control Conference*, 502–510.

Hoy, M., Matveev, A.S., and Savkin, A.V. (2015). Algorithms for collision-free navigation of mobile robots in complex cluttered environments: A survey. *Robotica*, 33(3), 463–497.

Johansen, T., Perez, T., and Cristofaro, A. (2016). Ship collision avoidance and colregs compliance using simulation-based control behavior selection with predictive hazard assessment. *IEEE transactions on intelligent transportation systems*, 17(12), 3407–3422.

Löfberg, J. (2004). YALMIP: A toolbox for modeling and optimization in MATLAB. In *Proc. of the CACSD Conference*.

Matveev, A.S., Teimoori, H., and Savkin, A.V. (2011). A method for guidance and control of an autonomous vehicle in problems of border patrolling and obstacle avoidance. *Automatica*, 47(3), 515 – 524.

Matveev, A., Hoy, M., and Savkin, A. (2013). A method for reactive navigation of nonholonomic under-actuated robots in maze-like environments. *Automatica*, 49(5), 1268 – 1274.

Sgorbissa, A. and Zaccaria, R. (2012). Planning and obstacle avoidance in mobile robotics. *Robotics and Autonomous Systems*, 60(4), 628–638.

Sontag, E.D. (1999). *Nonlinear Feedback Stabilization Revisited*, 223–262. Progress in Systems and Control Theory. Birkhäuser.

Tzafestas, S.G. (2013). *Introduction to Mobile Robot Control*. Elsevier.

Wiig, M., Pettersen, K., and Krogstad, T. (2019). Collision avoidance for underactuated marine vehicles using the constant avoidance angle algorithm. *IEEE Transactions on Control Systems Technology*, 28(3), 951–966.

Wiig, M., Pettersen, K., and Krogstad, T. (2020). A 3D reactive collision avoidance algorithm for underactuated underwater vehicles. *Journal of Field Robotics*, 37(6), 1094–1122.